

## **Whole-Tibia Structure and Muscle-Bone Relationships in the Legs of Trained Long-Distance Runners. A Serial pQCT Study**

Feldman S<sup>1</sup>, Capozza R<sup>1</sup>, Mortarino P<sup>1</sup>, Yelin I<sup>1</sup>, Reina P<sup>1</sup>, Rittweger J<sup>2</sup>, Ferretti JL<sup>1</sup>, Cointry G<sup>1</sup>

<sup>1</sup>Center for P-Ca Studies ( CEMFoC ), Natl Univ of Rosario, Argentina;

<sup>2</sup>Inst for Biomed Res into Human Movement & Health, Manchester Metropol Univ, UK.

### **AIMS AND METHODS**

This study aimed to study the impact of a chronic, low-intensity, long-volume mechanical stimulation of the leg on tibia structure.

With that purpose, pQCT scans ( *XCT-2000, Stratec, Germany* ) were taken at regular intervals ( 5% of whole bone length each, no scan at the 50% site, 18 scans/leg ) in 15 trained long-distance runners ( 9 males ) aged 20-40yr, otherwise normal, and in 10 male and 10 female age-matched sedentary controls.

Indicators of bone mass ( cortical area, total & cortical BMC, ToA, ToC, CtC ), diaphyseal design (periosteal & endocortical perimeters, PeriC, EndoC; cortical thickness, CtTh; bending & torsion moments of inertia, MIs ), material "quality" ( partial-volume adjusted cortical vBMD, Adj-vCtD ) and strength ( Stress-Strain Index, SSI ), and muscle mass ( cross-sectional area, MA ) were determined in each scan as allowed.

Correlations between MIs (  $y$  ) and CtA ( *distribution/mass curves* ) or Adj-vCtD ( *distribution / quality curves* ) evaluated the efficiency of the architectural distribution of the cortical tissue as a function of its availability or "quality" ( mineralization ), respectively. These curves were regarded to assess the ability of bone *mechanostat* to optimize the diaphyseal design in order to control the bone's structural stiffness.

### **The chief questions to answer were:**

1. How much does long-distance running practice improves the mineralized mass, cortical material quality, and diaphyseal design and strength of the tibiae with respect to the skeletal status of sedentary people as assessed by pQCT technology in voluntarily recruited individuals.
2. Whether the functional status of bone mechanostat could or not have a role in the determination of these effects.
3. Whether the eventual improvements achieved by long-distance running are or not associated to the mass or the usage of the calf muscles.

### **RESULTS**

All CtA, ToC, PeriC, CtTh, MIs, SSI and MA values were significantly larger in males than females.

Despite their high-volume physical activity, long-distance runners did not show larger MA than controls. Instead, runners had larger CtC, MIs and SSI than controls, either in absolute values or adjusted to a same MA value (  $p < 0.001$  ), especially close to the mid-diaphyses.

However, the Adj-vCtD, always higher in females than males, was reduced in both groups of runners (  $p < 0.01$  ).

Nevertheless, d/m and d/q curves showed always larger MIs' values for runners for the same CtC or Adj-vCtD values, respectively (  $p < 0.001$  ).

## **INTERPRETATION**

Results suggest that bone mass and structure are achieved as a function of the intensity and volume of the mechanical use of the regional muscles, rather than their mass.

However, when the volume of that activity is exaggerated, the intrinsic stiffness of cortical bone (known to be proportional to vCtD) can be impaired by microdamage caused by excessive remodeling.

Nevertheless, the architectural distribution of cortical tissue would be sensitive to exercise volume, perhaps to compensate for the reduction of bone material quality in the runners.

Long-distance runners would tend to show both a reduced “quality” and a better architectural distribution of cortical bone in their tibiae. As a result, runners’ tibiae tend to be more robust than those of their sedentary controls for a similar cortical mass or quality, or for the same calf muscle mass, perhaps as a function of the volume of mechanical use of the legs.

This mechanism would improve bone design, but not necessarily bone strength (SSI calculation does not capture bone microdamage), as long as runners’ tibiae may tend to suffer fatigue fractures.

All these results are in complete agreement with Frost's *Mechanostat* Theory.

**Ovariectomy Stimulates Midshaft Femur Endocortical Bone Formation in Rats but Not Mice** Andrea Y. Thompson, Jean-Pierre Revelli, Wendy Xiong, Jeff Liu, Sabrina Jeter-Jones, Melanie K. Shadoan and Robert Brommage

Department of Metabolism, Lexicon Pharmaceuticals, The Woodlands, TX, USA

Endocortical bone is lost during aging in humans and following ovariectomy in rodents. Therapies that stop this bone loss (bisphosphonates) and stimulate endocortical bone formation (teriparatide) promote cortical bone strength and fracture prevention.

We employed triple fluorochrome labeling protocols to evaluate the effect of ovariectomy on endocortical bone formation in C57BL/6 mice (16 weeks-old at surgery) and Fischer 344 rats (40 to 43 weeks-old at surgery). Calcein (10 mg/kg), alizarin complexone (20 mg/kg) and demeclocycline (30 mg/kg,) were injected at intervals of 7 days (mice) or 10 and 11 days (rats), with necropsy 7 days after the last label. Femurs were embedded in methacrylate using a 7-day protocol and sectioned to ~80  $\mu\text{m}$  thickness using a Leica SP1600 Saw Microtome. Histomorphometric measurements were made using OsteoMeasure (means  $\pm$  SEM shown).

Surgery/Species	Age (weeks)	N	CtTh ( $\mu\text{m}$ )	BFR/EcS ( $\mu\text{m}^3/\mu\text{m}^2/\text{day}$ )	
				Interval 1	Interval 2
Sham/Mouse	25 to 27	13	239 $\pm$ 4	0.33 $\pm$ 0.04	0.27 $\pm$ 0.03
OVX/Mouse	25 to 27	10	220 $\pm$ 4	0.26 $\pm$ 0.05	0.31 $\pm$ 0.05
Sham/Rat	84 to 87	13	635 $\pm$ 9	0.22 $\pm$ 0.04	0.26 $\pm$ 0.04
OVX/Rat	84 to 87	14	582 $\pm$ 9	0.78 $\pm$ 0.05	0.82 $\pm$ 0.05

The three fluorochromes gave similar values for single-labeled surface, indicating equivalent incorporation. Ovariectomy reduced cortical thickness by 8% in both species and stimulated midshaft femur endocortical bone formation 3.4-fold in rats, but had not in mice. Increases in mineralizing surface (2-fold) and mineral apposition rate (1.8-fold) were observed in ovariectomized rats.

## Osteocyte Lacunar Properties in Ovariectomized Rats with and without PTH(1-34) Treatment

D.B. Kimmel<sup>2</sup>, T. Fong<sup>3</sup>, S. Candell<sup>3</sup>, J. Coats<sup>3</sup>, M. P. Akhter<sup>2</sup>, T. J. Wronski<sup>1</sup>

<sup>1</sup>Department of Physiological Sciences, University of Florida; Gainesville, FL

<sup>2</sup>Osteoporosis Research Center, Creighton University; Omaha, NE

<sup>3</sup>Xradia Inc.; Concord, CA

Existing laboratory-based 3D-imaging technology has difficulty resolving features the size of osteocyte lacunae (Ot.La) in intact bone specimens. Synchrotron-based 3D imaging (0.7 $\mu$ m pixel resolution [PR]) permits viewing whole Ot.La. 3D X-Ray microscopy, a laboratory-based method that also images at sub-micron resolution, could be useful. Parathyroid hormone (PTH) and estrogen deficiency influence Ot activity and may alter Ot.La size and number. Our purpose is to quantify Ot.La properties in ovariectomized (OVX) and OVX+PTH-treated rats.

Female rats aged 13wks were ovariectomized (OVX) or Sham-OVXd. After 6wks, OVX rats were treated SC for 16wks with 0 [Veh] or 0.05 mg/kg PTH(1-34) [PTH] 5d/wk. Tibiae and L2 vertebrae (L2V) were fixed in 10% PO<sub>4</sub>-buffered formalin for 24hrs, then stored in 70% ethanol. Histomorphometric studies showed typical PTH and OVX-related changes in proximal tibial cancellous bone. L2V (4/grp) were trimmed of all processes and embedded in methacrylate. Sagittal samples measuring 2mmX2mmX8mm were prepared and scanned (5 $\mu$ m PR) with a 3D X-Ray microscope. 3D images were reconstructed and a 0.9mm diameter sub-volume of interest (VOI) rich in trabecular bone was re-scanned at 0.5 $\mu$ m PR. 3D images of each VOI were analyzed by segmentation software (Ratoc; Tokyo, JP).

Based on frequency distribution (Fig. 1), Ot.La were defined as bone tissue voids >10 and <400 $\mu$ m<sup>3</sup>. Data are presented in the Table.

OVX+Veh rats had smaller and fewer Ot.La than Sham-OVX rats. OVX+PTH rats tended to have larger and more numerous Ot.La than OVX+Veh rats. These data, generally consistent with past reports, suggest that 3D X-Ray microscopy is a laboratory-based sub-micron imaging technique that can facilitate the study of osteocyte lacunar properties in rodent bone.

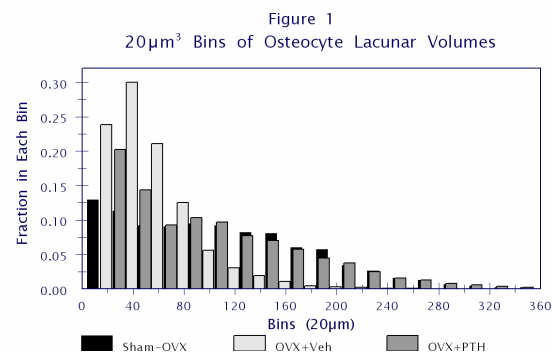


Figure 1. Frequency Distribution of Void Volumes in Bone Tissue. Note that >70% of voids in the OVX+Veh group have volumes less than 60 $\mu$ m<sup>3</sup>.

Variable	Units	Sham-OVX	OVX+Veh	OVX+PTH
BV/TV	%	38.3 $\pm$ 9.2 <sup>o</sup>	24.2 $\pm$ 4.3	38.2 $\pm$ 5.7 <sup>o</sup>
Ot.LaD	mm <sup>-3</sup>	61718 $\pm$ 10115 <sup>o</sup>	42770 $\pm$ 10449	55670 $\pm$ 8152 <sup>p</sup>
iOt.LaV	$\mu$ m <sup>3</sup>	104.5 $\pm$ 35.9 <sup>o</sup>	45.4 $\pm$ 5.9	86.6 $\pm$ 32.5 <sup>o</sup>
$\Sigma$ Ot.LaV/BV	%	0.668 $\pm$ 0.323 <sup>o</sup>	0.197 $\pm$ 0.068	0.498 $\pm$ 0.235 <sup>p</sup>
(N=4) Mean $\pm$ SD; <sup>o</sup> diff from OVX+Veh (P<.05); <sup>p</sup> diff from OVX+Veh (P<.10)				
Bone Volume (BV); Total Volume (TV); Ot.La Density (Ot.LaD); individual Ot.La Volume (iOt.LaV); Total Ot.La Volume/Bone Volume ( $\Sigma$ Ot.LaV/BV)				

## Osteocyte Lacunar Properties in Adult Human Bone Evaluated by 3D X-ray Microscopy

M.P. Akhter<sup>1</sup>, S. Candell<sup>2</sup>, R. R. Recker<sup>1</sup>, T. Fong<sup>2</sup>, J. Coats, D.B. Kimmel<sup>1</sup>

<sup>1</sup> Osteoporosis Research Center; Creighton University, Omaha, NE

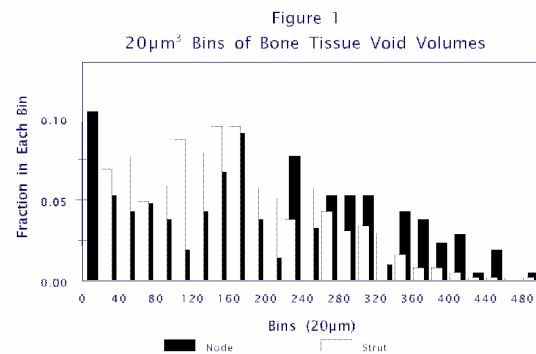
<sup>2</sup>Xradia Inc., Concord, CA

Though measurement of fracture site specific bone mass by densitometry currently explains much of the variation in bone strength, other measurable factors may contribute. Osteocyte lacunar (Ot.La) properties are seldom studied due to their small size and methodologic issues. As Ot number or size increases, local bone tissue strength may decline due to loss of mass. As Ot number or size decreases, local bone tissue strength may also decline due to the loss of void space that limits crack propagation. Thus, *any* minute, coordinated change across all Ot.La could negatively influence bone strength.

A laboratory-based method that images Ot.La in 3D with sufficient resolution to reliably quantitate their density and volume could enhance the ability to non-destructively measure bone strength. Current laboratory-based imaging technology has difficulty resolving structures the size of Ot.La in intact bone specimens. Our purpose is to quantify Ot.La properties in various bone microarchitectural regions in adult human bone.

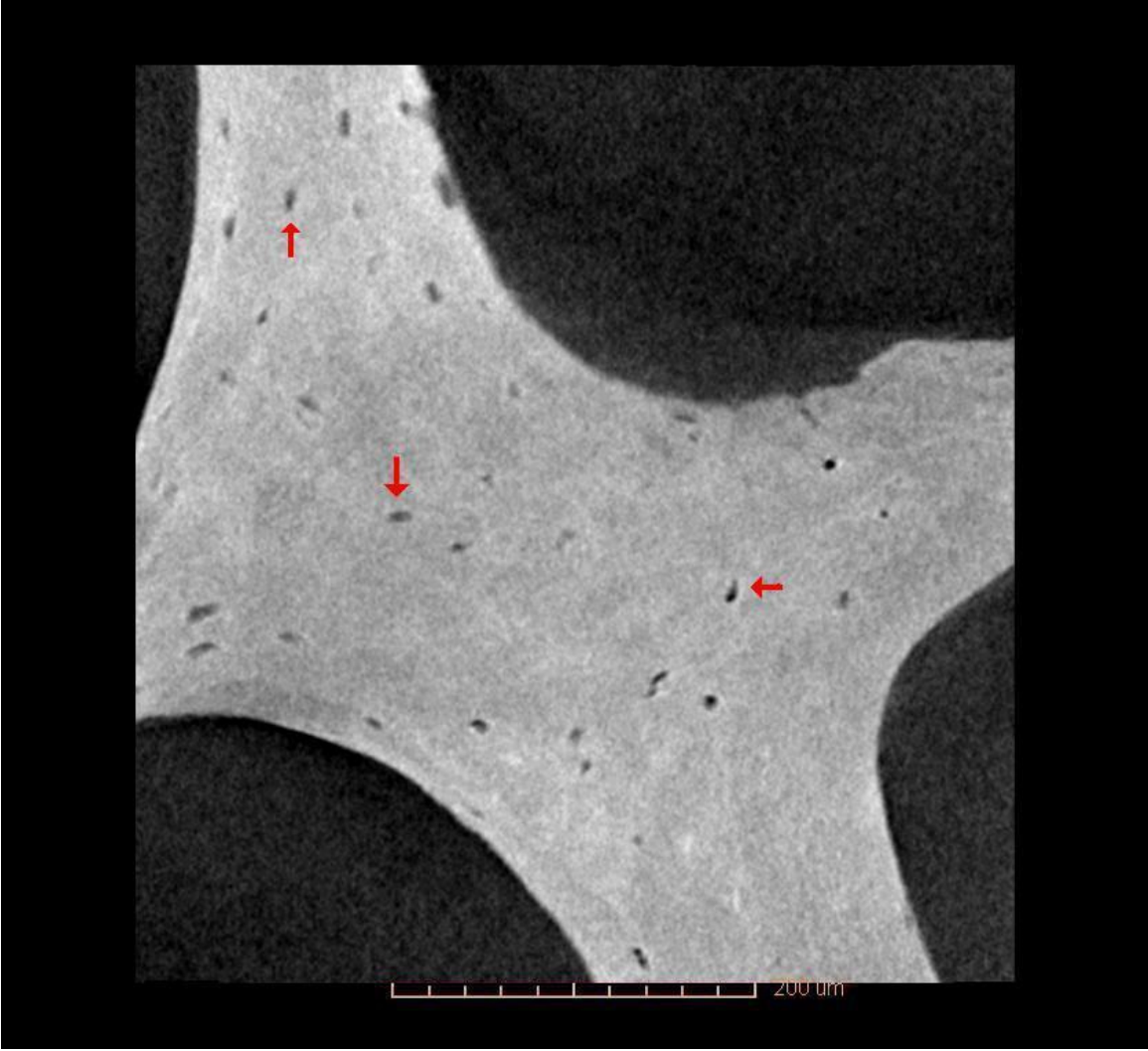
A transilial bone biopsy specimen from a healthy post-menopausal woman was embedded undecalcified in methacrylate. Sections were prepared for histomorphometric evaluation. The remainder of the plastic-embedded specimen was trimmed to 2mm X 2mm X 8mm and scanned initially at 5µm pixel resolution [PR] with a 3D X-ray microscope. 3D images were reconstructed. Cylindrical volumes of interest (VOIs) (~1mm diameter X 0.7mm long) that contained trabecular nodes, trabecular struts, or the cortex were identified and scanned at 0.5µm PR. 3D images of each VOI were reconstructed and analyzed by segmentation software (Ratoc; Tokyo, JP).

A frequency distribution is shown (Figure 1) and means are shown (Table). Each VOI was analyzed three times. The coefficients of variation for iOt.LaV, Ot.LaD, and Ot.LaV/BV were 3-6%. While iOt.LaV varied little (~9%) among the three regions, Ot.LaD was 45% higher (nodes) and 17% higher (struts) than in the cortex. Struts were 65% more porous than the cortex. The general dimensions here compare favorably to Ot.La measurements taken by 2D methods.



Variable	Units	Trab Node	Trab Strut	Cortex
Volume (BV)	mm <sup>3</sup>	0.0160	0.0067	0.0026
Ot.La#	#	514	174	59
Ot.LaD	mm <sup>-3</sup>	32272	26062	22232
iOt.LaV	µm <sup>3</sup>	237±125	216±111	227±124
ΣOt.LaV/BV	%	0.75	0.56	0.46
Ot.La#-# of Ot analyzed; Trab-trabecular; mean±SD				
Ot.La density (Ot.LaD), individual Ot.La volume (iOt.LaV), and total Ot.La volume/bone volume (ΣOt.LaV/BV) (lacunar-related porosity)				

Figure 2. 0.5µm PR slice from trabecular node. Note uneven distribution of Ot.La (arrows).





## IMAGING BONE MORPHOLOGY TO SUBMICRON AND NANOSCALE RESOLUTION WITH LAB BASED CT

S.H. Lau<sup>1\*</sup>, Lynda Bonewald<sup>2</sup>, Tiffany Fong<sup>1</sup>, Luke Hunter<sup>1</sup>, Pierre Lefebvre<sup>1</sup>, Jeff Gelb<sup>1</sup>

<sup>1</sup> Xradia Inc, 5052 Commercial Circle, Concord, CA 94520, USA

<sup>2</sup> School of Dentistry, University of Missouri at Kansas City, Kansas City, United States

email: shlau@xradia.com

We describe a **Multiscale 3D Bioimaging technique** using a suite of novel lab based x-ray micro and nanotomography system to characterize whole organ to its tissue, cells and subcellular structures with spatial resolution from 20 microns to 50 nm. Preliminary results on calcified, soft tissue and bioscaffolds demonstrated that Imaging resolution and contrast from the laboratory systems are very similar to published results obtained from x-ray micro and nanotomography with synchrotron radiation sources. Examples of 3D imaging of murine and human bones to visualize and quantify osteocyte lacunae-canaliculi in 3D (fig 1 and 2 ) for bone remodeling and osteoporosis research and its comparison to synchrotron tomography and SEM data is shown.

With Phase contrast techniques, the laboratory based tomography systems are also capable of high contrast imaging of soft tissue and biomaterials with and without contrast agents. Examples in ligament imaging within calcified tissue and bioscaffold at submicron resolution will be illustrated.

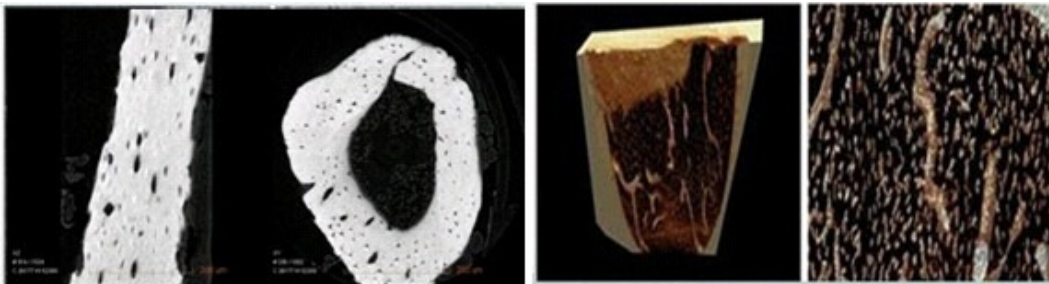


Fig 1. Submicron tomography of mouse femur showing osteocyte lacunae-vasculature distribution with Lab based MicroXCT @ 0.5 um voxel

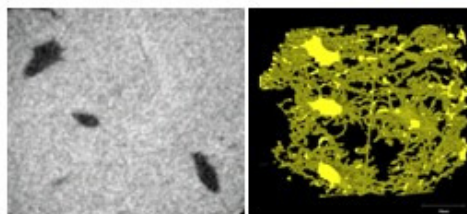


Fig 2. Nanotomography of mouse femur showing osteocyte lacunae canaliculi network with Lab based nanoXCT @ 60 nm voxel

**Keywords:** X-ray computed tomography, Multiscale 3D Imaging, Osteocyte lacunae characterization, Osteocyte canaliculi network, mouse and human bone biopsy

## Whole Bone Marrow Aspirate (BMA) for the Repair of Bone

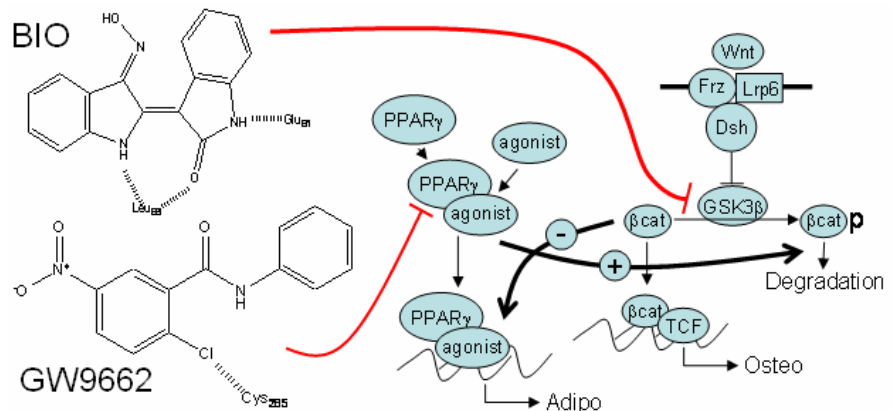
H. Wayne Sampson<sup>1,3</sup>, Carl Gregory<sup>2</sup>, Christopher Chaput<sup>3</sup>, and Suzanne Zeitouni<sup>1</sup>

<sup>1</sup>Departments of Systems Biology & Translational Medicine and <sup>2</sup>Molecular & Cellular Medicine  
The Texas A&M Health Science Center, College of Medicine, Temple, TX 76502  
And <sup>3</sup>Department of Surgery (Orthopedic Division) Scott & White Hospital

Recent evidence demonstrates that some current strategies to enhance bone formation in critical-gap fractures and bone graft procedures with bone morphogenetic proteins can cause significant and even life threatening complications (Robin et al., 2010). We report on our efforts to enhance healing by activating whole bone marrow preparations with a Wnt signaling modulator that drives the mesenchymal stem cells (MSCs) of the marrow towards osteogenesis. We predict that this treatment will enhance the osteogenic capacity of whole bone marrow.

Our strategy involves a simple iliac crest aspirate performed at the point of care (surgery), concentration of the whole bone marrow using a closed concentrator system, then rapid stimulation the cells with a glycogen synthetase kinase 3 $\beta$  (GSK3 $\beta$ ) inhibitor (bromo-indirubin-monooxime, or BIO). These procedures will allow for “back-table” activation at the point of care and will not require being taken to an outlying laboratory for expansion.

We and others observed that canonical Wnt signaling is essential for the progression of an hMSC to an early osteoblast (reviewed in Gregory *et al.* 2006, Krause *et al.* 2010). Furthermore, we found that by inhibiting either GSK3 $\beta$  or by inhibiting the master regulator of adipogenesis, peroxisome proliferator activated receptor- $\gamma$  (PPAR $\gamma$ ), we can enhance osteogenic potential by hMSCs through acceleration of Wnt signaling. Inhibition of these targets enhance Wnt signaling by 2 mechanisms; by directly inhibiting phosphorylation of  $\beta$ -catenin or by reducing inhibitory crosstalk from the adipogenic PPAR $\gamma$  axis (Gunn et al, 2005; Hadjiargyrou et al., 2002; Haynesworth et al., 1992). In this poster, we report on the effects of GSK3 $\beta$  inhibition through the action of the nucleotide analogue, BIO.



In initial experiments (Krause et al. 2010), we tested the ability of BIO to enhance early and late stages of osteogenesis. When hMSCs were treated with BIO, the early osteogenic markers alkaline phosphatase (ALP) and osteoprotegerin (OPG) were upregulated in a dose dependent manner. Furthermore, we found that BIO expression also reduced secretion of the Wnt inhibitor Dkk-1. Given that BIO enhanced expression of early osteogenic markers, we then assayed for late differentiation. In this series of assays, we pre-incubated the MSCs for 10 days in the presence of osteoinductive media for 10 days, then added media containing dexamethasone to initiate a biomineralizing phenotype, similar to that seen when osteoblasts generate bone. The calcified matrix generated in the culture dish was then stained with the calcium binding dye alizarin red. The dye bound was quantified by a series of extractions, followed by spectrophotometric quantification (Gregory *et al.* 2004). BIO caused an increase in the ability of the MSCs to deposit a mineralized matrix in a dose dependent manner. This effect seems to be generally irreversible because when BIO is withdrawn at day 10 and only dexamethasone is included in the mineralizing base media, the effect can still be seen. In subsequent experiments, we found that as short as 1 hr transient pre-exposure to BIO prior to osteogenic induction was sufficient to enhance differentiation



of the hMSCs in culture, thereby validating the use of BIO for conditioning the osteogenic component of unfractionated mononuclear preparations of bone marrow.

We have attempted to identify an appropriate scaffold that will create a niche for osteogenic cells in proximity of the healing critical-gap fractures (Chaput et al., 2010, Wright et al., 2010). The scaffold will help confine the cells to the site, provide the necessary solid-phase support essential for osteogenic differentiation, and potentially carry growth factors while newly administered cells achieve homeostasis *in vivo*. Previously, with long bone fractures, we tested a bioresorbable PLA:DX:PEG polymer for 6 weeks, which permitted some poorly directed healing, but surprisingly initiated marrow osteolysis in many of the cases (Wright et al., 2010). Following the addition of BIO to the polymer, we were successful in producing healing in the fracture gap, but it was un-directed in an orientation that appeared to be leakage of the material from the site. We have not used this polymer in the cranial defect, but similar results with craniofacial bones have been identified by Robey and Bianco (2006). These results with long bone fractures emphasized the fact that we need to administer the cells in a more biocompatible scaffold that provides a “niche” for osteogenic cells to grow. For this purpose, we have developed a number of candidate scaffolds with distinct properties that can be used in conjunction with each other. For instance, an ultrafine bone powder that adheres to freeze dried cancellous bone chips will create porosity and cell retention similar to a cancellous autograft. Alternatively, a synthetic calcium-phosphate silica-based ceramic scaffold specially constructed to mimic trabecular architecture was combined with particulate collagen to mimic the allograft scaffold. We have also been working on the development of a scaffold made of the extracellular matrix created by osteogenically cultured MSCs, which provides an excellent environment for MSCs during healing of calvarial lesions and therefore should have the same positive effect on concentrated bone marrow. In order to localize the cells within the scaffold, we used a plasma clot (Krause *et al.* 2010).

The results of this project can be easily translated into clinical projects with humans. Whether the agents are directly administered, or used to condition cultures of hMSCs, we believe this technology can be applied to non-union fracture treatment, repair of bone-implant interfaces, systemic diseases of the skeleton, and probably spinal fusion, with the capability to compete with more established osteogenic repair strategies.

Chaput, C.D., Wright, C. A., Souder, C. D., Kummerfeld, D. A., Williams, J. F., Sampson, H.W. An Intramedullary Critical Size Defect Model for Non-Union in Rats. JOT (submitted)

Gregory, C.A., Gunn, W. G., Piester, A. and Prockop, D. J. (2004) An Alizarin red based method for the assay of mineralization by adherent cells in culture. Comparison with cetylpyridinium chloride extraction. *Anal. Biochem.* 329, pp. 77-84.

Gregory, C. A., Green, A., Lee, N., Rao, A. and Gunn, W. (2006b) The Promise of Canonical Wnt Signaling Modulators in Enhancing Bone Repair. *Drug News Pers.* **19**, 445-452.

Gunn, W. G., Conley, A., Deininger, L., Olson, S. D., Prockop, D. J. and Gregory, C. A (2005) A Crosstalk between Myeloma Cells and Marrow Stromal Cells Stimulates Production of DKK1 and IL-6: A Potential Role in the Development of Lytic Bone Disease and Tumor Progression in Multiple Myeloma. *Stem Cells.* **24**, 986-991

Hadjiargyrou, M., Lombardo, F., Zhao, S., Ahrens, W., Joo, J., Ahn, H., Jurman, M., White, D. W. and Rubin, C. T. (2002) Transcriptional profiling of bone regeneration. Insight into the molecular complexity of wound repair. *J. Biol. Chem.* **277**, 30177-30182.

Haynesworth, S. E., Goshima, J., Goldberg, V. M. and Caplan, A. I. (1992) Characterization of cells with osteogenic potential from human marrow. *Bone*. **13**, 81-88.

Krause U, Harris S, Green A, Ylostalo J, Zeitouni S, Lee N, Gregory C A. (2010) Pharmaceutical modulation of canonical Wnt signaling in multipotent stromal cells for improved osteoinductive therapy. Proc. Natl. Acad. Sci. USA. **107**:4147-4152.

Robey, P., Bianco, P. (2006) The use of adult human stem cells in rebuilding the human face. *JADA* **137**, 961-972.

Robin, B.N., Chaput, C.D. Zeitouni,S., Sampson, H.W. Cytokine Mediated Inflammatory Reaction Following Posterior Cervical Decompression and Fusion Associated With rh-BMP-2: a Case Study. *SPINE* (in press)

Wright, C., Chaput, C., Ward, R., Gregory, C., Schwartz, C.J. Sampson, H.W. Osteolysis and Inflammatory Response with PLA:DX:PEG in a Segmental Defect Rat Model. *JOT* (submitted)

## **Partial Weightbearing Does not Prevent Bone loss Compared to Non-Weightbearing Model**

Florence Lima<sup>1</sup>, Joshua M Swift<sup>1</sup>, Elizabeth S Greene<sup>1</sup>, Matthew R Allen<sup>2</sup>, Brandon R Macias<sup>1</sup> and Susan A Bloomfield<sup>1,3</sup>

<sup>1</sup>Department of Health and Kinesiology, Texas A&M University, College Station, TX 77843

<sup>2</sup>Department of Anatomy and Cell Biology, Indiana University, Indianapolis, IN 46202

<sup>3</sup>Intercollegiate Faculty of Nutrition, Texas A&M University, College Station, TX 77843

While the effects of unloading are well-described in animal models simulating space, the effects of partial weightbearing, as expected on the moon and Mars, have yet to be quantified. We hypothesized that mice exposed to 1/6th gravity (G/6) and 1/3rd gravity (G/3) will experience significant reductions in cancellous bone structure and bone formation vs. 1 gravity (1G) controls, but the magnitude of these changes would be less than in fully unloaded (0G).

4-mo-old female BALB/cByJ mice were randomly assigned to cage control (1G), traditional tail suspension (0G), G/6, or G/3 groups for a 21-day suspension protocol. The partial G model is a modification of the traditional tail suspension providing graded chronic reductions in weightbearing quadrupedal loading in mice. *Ex vivo* Micro-CT scans (microCT; Skyscan 1172) on day 21 were performed to assess bone structural properties, and dynamic bone histomorphometry assessed bone formation on the distal femur.

Compared to the 1G group, distal femur BV/TV, Tb.Th, and Tb.N were lower (-24%, -12%, -14%, respectively) by 21d in the 0G, G/6 and G/3 groups with no difference between groups. Tail suspension induced significant suppression of bone formation (BFR/BS: -57%) and mineralized surface (MS/BS: -49%) in the distal femur metaphysis with similar magnitude in the G/6 (BFR/BS: -49%, MS/BS: -43%), and G/3 groups (BFR/BS: -46%, MS/BS: -39%).

These data suggest that partial weightbearing, as high as G/3, does not prevent the significant deterioration of cancellous bone observed in the 0G condition and did not protect against the decrease of bone formation.

*Funded by NSBRI through NASA Cooperative Agreement NCC 9-58.*

## **Sclerostin antibody acts as a positive anabolic agent for peri-implant bone in ovariectomized rats**

Irish, J; Viridi, AS; Sena, K; Liu, M\*, Ke, HZ\*, Sumner, DR

Rush Medical College, Chicago, IL, \* Amgen Inc, Thousand Oaks, CA

Osteoporosis has long been recognized to be the result of an imbalance in normal bone metabolism in favor of catabolism. The protein sclerostin, derived from the SOST gene, inhibits bone formation. Sclerostin antibody has been shown to have an bone anabolic effect in a rat osteoporotic model (Li et al. J Bone Miner Res. 2009;24(4):578-88). We hypothesized that systemic sclerostin antibody in a rat implant fixation model would result in increased peri-implant bone formation. A total of 24 female Sprague-Dawley rats underwent either sham ovariectomy (Sham, n = 12) or ovariectomy (Ovx, n = 12). Five months later, each rat received bilateral titanium femoral implants. The rats were then treated with twice weekly saline vehicle or sclerostin antibody (Scl-AbIII, 25 mg/kg) subcutaneous injections for 12 weeks (n = 6 rats in each group). After sacrifice, the bone volume to total volume ratio (BV/TV) was evaluated in a region of interest between the endocortical surface and the implant superior to the growth plate by  $\mu$ CT.

An analysis of variance showed that both of the fixed effects (sham vs. Ovx and vehicle vs. Scl-AbIII treatment) were significant ( $p < 0.001$ ). In the sham groups, BV/TV increased from 33.5% to 75.7% with Scl-AbIII treatment, whereas in the ovx group, BV/TV increased from 13.1% to 24.2% with Scl-AbIII treatment. This difference in response between sham and ovx rats was significant. The present study showed that sclerostin antibody has the ability to increase bone volume around an implant in a rat model of postmenopausal osteoporosis.

Acknowledgements: Rush Dean's Fellowship

## Bone Structural Properties Explain Mechanical Deficits of Lumbar Vertebrae in Male Diabetic Rats

Kathleen M. Hill, Maxime A. Gallant, Susan Reinwald, David B. Burr  
Department of Anatomy and Cell Biology, Indiana University School of Medicine, Indianapolis, IN

Type 2 diabetes mellitus (T2DM) patients have greater risk for fracture despite normal or high BMD compared to non-diabetic persons. Therefore, methods beyond BMD are needed to determine fracture risk in diabetic patients. Our objective was to determine if bone structural properties predict the differences in bone mechanical properties observed between ZDSD and non-diabetic CD rats (controls).

Sixteen-wk-old ZDSD male rats were fed a high-fat diet to induce T2DM, and sacrificed 14-wk later. Structural properties of lumbar vertebrae (L4) were determined by DXA and  $\mu$ CT, and mechanical properties were obtained from axial compression.

Independent t-tests were used to detect differences in structural and mechanical properties between groups. Multiple linear regression and stepwise selection were used to identify structural predictors of mechanical properties.

ZDSD had lower ultimate force (UF), energy to UF, yield force, ultimate stress (US), and toughness (all  $p < 0.0001$ ) compared to controls. L4 ventral cortical thickness (Ct.Th) was lower in ZDSD compared to controls ( $p < 0.0001$ ) and predicted 88% and 67% of the variation in UF and US, respectively (both  $p < 0.0001$ ). BMD predicted an additional 3% of the variation in UF ( $p < 0.0001$ ). After accounting for ventral Ct.Th, there were no differences in UF or US between ZDSD and controls.

Our results agree with literature in humans showing anterior (ventral) Ct.Th and BMD are strong predictors of vertebral strength. We show that these structural measures account for the differences in bone strength between diabetic and control rats. Therefore, non-invasive structural measures may be useful in identifying risk of fracture in diabetes.

**DEVELOPMENT OF A HISTOLOGICAL GRADING SCHEME FOR OSTEOARTHRITIS  
IN MICE** M. A. McNulty<sup>1</sup>, R. F. Loeser<sup>2</sup>, C. Davey<sup>3</sup>, C. Ferguson<sup>2</sup>, M. F. Callahan<sup>2</sup>, C. S. Carlson<sup>4</sup>;

<sup>1</sup> Rush University Medical Center, Chicago, IL, <sup>2</sup> Wake Forest Univ., Winston-Salem, NC, <sup>3</sup> Univ. of Minnesota, Minneapolis, MN, <sup>4</sup> Univ. of Minnesota, Saint Paul, MN **Abstract:**

Histological grading schemes that are used for osteoarthritis (OA) need to be improved in order to accurately characterize the severity of this disease. The purpose of this study was to develop a histological grading scheme to accurately assess the severity of OA in mice. This study utilized murine stifle joints from 5 studies (n=158 stifle joints) that included both surgically induced OA in young mice and naturally occurring OA in adult mice and represented a wide range of OA severities. Two representative midcoronal sections were selected for evaluation and stained with H&E and Safranin-O stains. Fifteen parameters composed of both quantitative and semi-quantitative measurements were evaluated in each tibial plateau of each stifle. All data was combined into one data set and evaluated using correlation analysis and Principal Components Analysis (PCA) by a statistician having no knowledge of the intervention groups. Correlation analysis revealed strong correlations in the medial tibial plateau ( $p < 0.0001$ ) between the two semi-quantitative parameters and 6 continuous parameters. Correlations were weaker in the lateral tibial plateau. Five factors were retained by PCA using data from the medial tibial plateaus, accounting for 74% of the total variance in the data. These grouped logically into factors describing articular cartilage structure, chondrocyte viability, subchondral bone, meniscus, and osteophytes. A comprehensive histological grading scheme was developed to describe joint changes of OA in mice. PCA allowed the generation of factors describing OA severity in the medial tibial plateau that had conceptual meaning



## **Mechanical loading during disuse produces robust increases in bone formation rate and reduced number of sclerostin-positive osteocytes**

<sup>1</sup>BR Macias, <sup>1</sup>JM Swift, <sup>2</sup>SD Bouse, <sup>2</sup>HA Hogan, and <sup>1</sup>SA Bloomfield

<sup>1</sup>Department of Health and Kinesiology, Texas A&M University, College Station, TX

<sup>2</sup>Department of Mechanical Engineering, Texas A&M University, College Station, TX

Mechanical loading modulates the osteocyte-derived protein sclerostin, a potent inhibitor of bone formation. We hypothesized that simulated resistance training (SRT) during rodent hindlimb unloading (HU) would reduce sclerostin-positive osteocytes while stimulating increases in cortical bone formation rate (BFR).

Male, Sprague-Dawley rats (6-mo-old) were randomly assigned to cage control (CC, n=12), hindlimb unloading (HU, n=12), and SRT groups (HU+SRT, n=12). Under anesthesia HU+SRT rats completed 4 sets of 5 electrically stimulated muscle contractions at 75% peak isometric strength. pQCT scans (days -1 and 28) were performed to assess cortical bone structural properties, and dynamic bone histomorphometry assessed bone BFR at mid-shaft tibial surfaces. Standard immunohistochemical procedures with sclerostin primary antibody (1:250, R&D Systems) were performed on mid-diaphyseal tibia to quantify sclerostin positive osteocytes.

Normalized to CC, the proportion of sclerostin-positive osteocytes was significantly higher (121%) in the HU group compared to the HU+SRT group (30%). Tibial midshaft cortical BMC, cortical area, and cross-sectional moment of inertia were significantly larger in the HU+SRT but did not change in the HU group after 28 days. Periosteal BFR was 56% lower in HU rats versus CC animals. However, we observed a 2.6- and 14-fold increase in periosteal and endocortical BFR, respectively, in HU+SRT versus CC rats.

These data demonstrate that a minimum number of high intensity muscle contractions, performed during disuse, suppress unloading-induced increases in sclerostin positive osteocytes and increases cortical bone formation.

Supported by NASA via contract to NSBRI NCC9-58-42 and NSBRI Graduate Student Training Fellowship NASA NCC 9-58 to BR Macias.